European Conference on Optical Communication (ECOC) 2022 © Optica Publishing Group 2022

Electro-Optic Frequency Response of Thin-Film Barium Titanate (BTO) from 20 to 270 GHz

Daniel Chelladurai[(1)], Manuel Kohli[(1)], Yannik Horst[(1)], Marco Eppenberger[(1)], Laurenz Kulmer[(1)], Tobias Blatter[(1)], Joel Winiger[(1)], David Moor[(1)], Andreas Messner[(1)], Clarissa Convertino[(2)], Felix Eltes[(2)], Yuriy Fedoryshyn[(1)] and Juerg Leuthold[(1)]

[(1)] Institute of Electromagnetic Fields (IEF), ETH Zurich, 8092 Zurich, Switzerland,
[(2)] Lumiphase AG, 8802 Kilchberg, Switzerland
daniel.chelladurai@ief.ee.ethz.ch, JuergLeuthold@ethz.ch

Abstract *The electro-optical frequency response of thin-film barium titanate (BTO) has been characterized in hybrid plasmonic-photonic phase shifters across the spectral range from 20 to 270 GHz. A flat frequency response was found. ©2022 The Author(s)*

Introduction

Materials with a large linear electro-optical coefficient across the largest possible frequency range are key enablers of future terahertz applications. They are needed in Mach-Zehnder modulators [1,2] and IQ modulators [3] to operate next generation networks, and they are essential in future millimetre and THz sensors or transceivers [4–6].

Ferroelectrics are a popular class of electro-optic (EO) materials due to their large Pockels coefficients [7,8]. Their inorganic nature is attractive for integration in electronic and photonic integrated circuits. Lithium niobate (LN) has been the traditional choice for commercial products. More recently its availability as LN-on-insulator wafers has led to impressive modulator demonstrations [9,10]. Alternatively, barium titanate (BTO) is gaining popularity because its Pockels coefficient is reported to be an order of magnitude larger than LN and has also recently become available as BTO-on-insulator substrates [11–14]. In each of these demonstrations, however, the measured frequency response has been limited to < 70 GHz except for [14], where the device was characterized up to 150 GHz. Yet, the material response was not completely separated from the device's electrical response.

Previous work on the frequency response of BTO has predicted roll-offs in the Pockels coefficients of ferroelectrics at characteristic frequencies relating to piezoelectric, ionic and electronic responses to external electric fields [15]. Some evidence of this drop has been observed in experiments [12,14,16] within the first 20-30 GHz. Apart from these experiments, other work has been dedicated to measuring dispersion in BTO's dielectric constant which can be linked to its nonlinearity through Miller's rule [17]. Measurements of dielectric relaxations in BTO have shown a drop in the dielectric constant in the sub-GHz range before stabilizing in the low-GHz range [18–20]. Above these frequencies the dielectric and electro-optic properties are expected to remain relatively constant until optical phonon frequencies above 1 THz [15,21]. Beyond theory guided assumptions, the range from 70 GHz to 1 THz is largely unexplored.

In this work we measure the electro-optic frequency response of BTO between 20 GHz and 270 GHz. We achieve this by measuring hybrid plasmonic-photonic phase-shifters where BTO is used as the active material. Our measurements indicate that BTO a flat electro-optic response.

Phase Shifter Design

We designed hybrid plasmonic-photonic phase shifters based on metal-loaded waveguides [22]. Fig. 1(a) shows a schematic of a typical device's cross-section. The device was fabricated on the BTO-on-insulator platform provided by Lumiphase. The oxide layer separating the BTO and the metals was deposited with plasma-enhanced chemical vapor deposition. The gold electrodes were deposited in a lift-off process using electron-beam evaporation. Amorphous silicon grating couplers were used to couple light in and out of the chip. Adiabatic mode converters served as an interface between the phase shifter and photonic

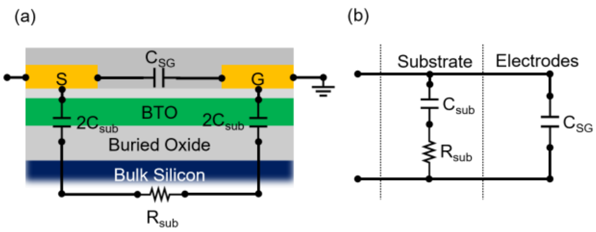

Fig. 1: (a) Schematic cross-section of the hybrid plasmonic-photonic phase shifter. "G" and "S" represent the ground and signal electrodes, respectively.
(b) Equivalent circuit representation of the phase shifter.

waveguides.

The design benefits from the metals serving as electrodes and as waveguides, similar to plasmonic slot waveguides [1,12]. This allows for a smaller separation between the metals in comparison to photonic modulators and leads to larger applied electric fields for nonlinear optical effects. Unlike the plasmonic slot waveguides, however, this design avoids an interface between the metal and the electro-optic material. Avoiding interfacial effects is important because they may modify the in-device Pockels coefficient [11,12]. We used short phase shifters of only 50 µm in length such that the electrodes are short enough to be treated as electrical lumped elements. This eliminates the influence of RF propagation loss and RF-optical velocity mismatch on the electro-optic response. BTO's large electro-optic coefficient gives a modulation response in the short device that is efficient enough to be measured with the technique of comparing sideband powers to the carrier power in an optical spectrum analyzer (OSA).

Measurement Method

We use optical spectrum analysis to measure the modulation efficiency of the phase shifters. Phase modulation generates two sidebands around the carrier frequency at $\omega_0 \pm \omega_\mathrm{m}$ where ω_0 is the carrier frequency and ω_m is the modulating frequency. The ratio between the carrier peak and the first sidebands is related to the modulator's V_π and therefore its efficiency [23]. Eq. (1) indicates that the peak-to-sideband ratio (P2SB) scales approximately quadratically with the inverse of V_π in the small signal limit.

$$\frac{I(\omega_0 \pm \omega_\mathrm{m})}{I(\omega_0)} \approx \left(\frac{\pi}{2}\frac{V_\mathrm{m}}{V_\pi}\right)^2 \qquad (1)$$

The carrier and sideband intensities are represented by $I(\omega_0)$ and $I(\omega_0 \pm \omega_m)$, respectively. V_m is the peak drive voltage of the modulating signal. A modulator's V_π is inversely related to the Pockels coefficient of the electro-optic material [24]. Thus, the P2SB scales approximately quadratically with the Pockels coefficient. After normalization of the driving voltage delivered to the phase shifter at each frequency, we can infer the electro-optic response of BTO through the P2SB. The P2SB's quadratic dependence on the Pockels coefficient lends extra sensitivity to the measurement of any changes in the material response.

To measure the frequency response we generated modulating signals over the full 20-270 GHz range with three different experimental configurations. Fig. 2. shows the general configuration of the measurement setup where the only difference between each measured frequency band is the method of generating the RF signal. From 20 to 70 GHz we use an analog signal generator. From 70 GHz to 110 GHz, we use the same signal generator but fed the analog signal into a 6x frequency multiplier followed by an amplifier. From 110 GHz to 180 GHz, we use the signal generator fed into a 3x frequency multiplier followed by an amplifier. Finally, from 200 GHz to 270 GHz we use optical heterodyning into a UTC photodiode followed by an amplifier. The method is described in further detail in [25].

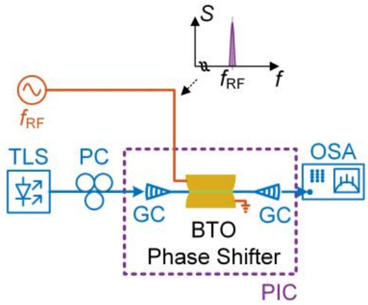

Fig. 2: Schematic representation of the measurement configuration.

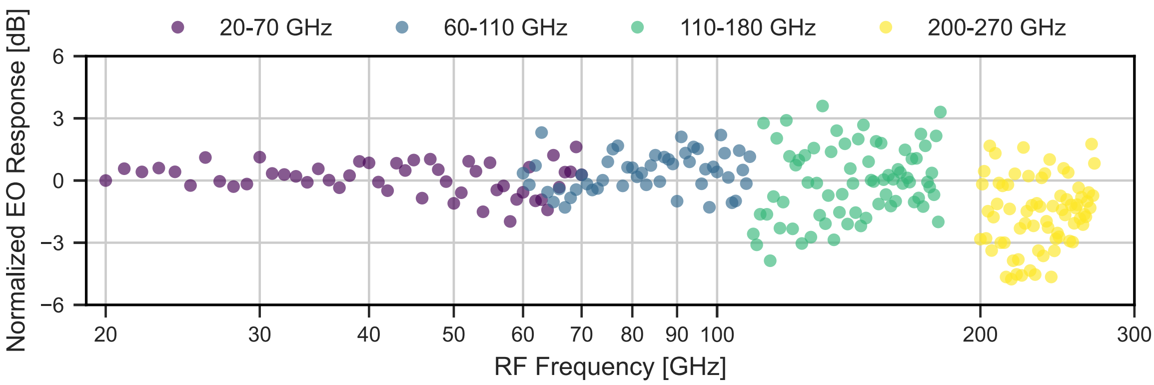

Fig. 3: Measured frequency response of BTO. The colors represent different measurement setups used to measure partial frequency ranges.

Measured Frequency Response

The measured frequency response of the BTO phase shifter is presented in Fig. 3. The P2SB is calculated from the raw spectra measured by the OSA and then corrected based on calibration measurements of the modulating signal's power. The calibration measurements include losses incurred in RF cables/waveguides, connectors and probes as well as the reflection of the driving signal at the device.

Below we discuss the calibration in more detail. In typical plasmonic modulators, the device may be assumed to be an open circuit and the driving signal is completely reflected at the device leading to a doubling of the voltage across the electrodes. However, here we have some RC-limitations that will reduce the voltage across the electrodes at higher frequencies. An equivalent circuit model of the device is depicted in Fig. 4(b). To find fitting parameters of the equivalent circuit we measured the S_{11} parameter of the phase shifter using a vector network analyzer (VNA) from 10 GHz to 50 GHz. The frequency range was limited by available equipment. The best fit was obtained with C_{SG} = 21.9 fF, C_{sub} = 18.3 fF and R_{sub} = 330 Ω. The fitted model was then used to extrapolate the reflection coefficient Γ up to 300 GHz as shown in Fig. 4(a). The extrapolated curve from the measured results was further verified by a finite element simulation of the device. The result of this simulation is also plotted in Fig. 4(b). We attribute the difference between the circuit model and the simulation to the use of lossless dielectrics in simulation, which is not the case for the measured values used to fit the model. The modulating voltage delivered to the device is then determined by $V_{\text{in}}(1+\Gamma)$ where V_{in} is the voltage of the incoming wave to the device and Γ = S_{11} is the reflection coefficient. The extrapolated roll-off in the voltage across the electrodes of the device is plotted in Fig. 4(b). Finally, we used this model in combination with calibration data from the RF path to the device to normalize the electro-optic response. This effectively eliminates all contributions to the measured modulation response except for the electro-optic response of the BTO.

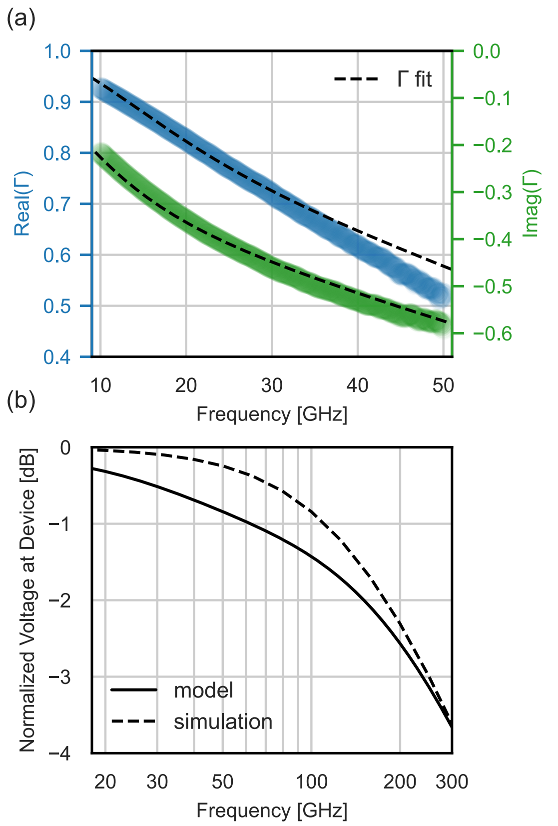

Fig. 4: (a) Measured reflection coefficient Γ (blue=real, green=imaginary) and the fitted values (black) obtained from the equivalent circuit. (b) Voltage at the device electrodes normalized to the voltage when Γ = 1 calculated from the fitted circuit model (solid) and from finite element simulation (dashed).

Conclusions

The first measurements on the electro-optic response of thin-film BTO extending from 20 GHz to 270 GHz have been performed. We fabricated hybrid plasmonic-photonic phase shifters using BTO as the active material and the measured material response shows minimal dispersion across the measured frequency range after accounting for the electrical response of the device. This indicates that the electro-optic response of BTO does not degrade in this frequency range. The present work lays a foundation to build upon for the design of THz electro-optic devices using inorganic materials.

Acknowledgements

We wish to thank the Cleanroom Operations Team of the Binnig and Rohrer Nanotechnology Center (BRNC) for their help and support. We also thank Martin Leich and Colombo Bolognesi for their contributions to high-frequency measurements. Some measurements in this study have been performed with LabExT, a free and open-source laboratory automation software available at https://github.com/LabExT/LabExT.

References

[1] C. Haffner, W. Heni, Y. Fedoryshyn, J. Niegemann, A. Melikyan, D. L. Elder, B. Baeuerle, Y. Salamin, A. Josten, U. Koch, C. Hoessbacher, F. Ducry, L. Juchli, A. Emboras, D. Hillerkuss, M. Kohl, L. R. Dalton, C. Hafner, and J. Leuthold, 'All-plasmonic Mach–Zehnder modulator enabling optical high-speed communication at the microscale', *Nature Photonics*, vol. 9, no. 8, pp. 525–528, 2015, doi: 10.1038/nphoton.2015.127.

[2] A. J. Mercante, S. Shi, P. Yao, L. Xie, R. M. Weikle, and

D. W. Prather, ‘Thin film lithium niobate electro-optic modulator with terahertz operating bandwidth’, *Optics Express*, vol. 26, no. 11, pp. 14810–14816, 2018, doi: 10.1364/OE.26.014810.

[3] W. Heni, Y. Fedoryshyn, B. Baeuerle, A. Josten, C. B. Hoessbacher, A. Messner, C. Haffner, T. Watanabe, Y. Salamin, U. Koch, D. L. Elder, L. R. Dalton, and J. Leuthold, ‘Plasmonic IQ modulators with attojoule per bit electrical energy consumption’, *Nature Communications*, vol. 10, no. 1, Art. no. 1, 2019, doi: 10.1038/s41467-019-09724-7.

[4] Y. Salamin, W. Heni, C. Haffner, Y. Fedoryshyn, C. Hoessbacher, R. Bonjour, M. Zahner, D. Hillerkuss, P. Leuchtmann, D. L. Elder, L. R. Dalton, C. Hafner, and J. Leuthold, ‘Direct Conversion of Free Space Millimeter Waves to Optical Domain by Plasmonic Modulator Antenna’, *Nano Letters*, vol. 15, no. 12, pp. 8342–8346, 2015, doi: 10.1021/acs.nanolett.5b04025.

[5] I.-C. Benea-Chelmus, T. Zhu, F. F. Settembrini, C. Bonzon, E. Mavrona, D. L. Elder, W. Heni, J. Leuthold, L. R. Dalton, and J. Faist, ‘Three-Dimensional Phase Modulator at Telecom Wavelength Acting as a Terahertz Detector with an Electro-Optic Bandwidth of 1.25 Terahertz’, *ACS Photonics*, vol. 5, no. 4, pp. 1398–1403, 2018, doi: 10.1021/acsphotonics.7b01407.

[6] Y. Horst, T. Blatter, L. Kulmer, B. I. Bitachon, B. Baeuerle, M. Destraz, W. Heni, S. Koepfli, P. Habegger, M. Eppenberger, E. D. Leo, C. Hoessbacher, D. L. Elder, S. R. Hammond, L. E. Johnson, L. R. Dalton, Y. Fedoryshyn, Y. Salamin, M. Burla, and J. Leuthold, ‘Transparent Optical-THz-Optical Link at 240/192 Gbit/s Over 5/115 m Enabled by Plasmonics’, *Journal of Lightwave Technology*, vol. 40, no. 6, pp. 1690–1697, 2022.

[7] M. Zgonik, P. Bernasconi, M. Duelli, R. Schlesser, P. Günter, M. H. Garrett, D. Rytz, Y. Zhu, and X. Wu, ‘Dielectric, elastic, piezoelectric, electro-optic, and elasto-optic tensors of $BaTiO_3$ crystals’, *Physical Review B*, vol. 50, no. 9, pp. 5941–5949, 1994, doi: 10.1103/PhysRevB.50.5941.

[8] M. Jazbinšek and M. Zgonik, ‘Material tensor parameters of $LiNbO_3$ relevant for electro- and elasto-optics’, *Applied Physics B*, vol. 74, no. 4, pp. 407–414, 2002, doi: 10.1007/s003400200818.

[9] C. Wang, M. Zhang, X. Chen, M. Bertrand, A. Shams-Ansari, S. Chandrasekhar, P. Winzer, and M. Lončar, ‘Integrated lithium niobate electro-optic modulators operating at CMOS-compatible voltages’, *Nature*, vol. 562, no. 7725, Art. no. 7725, 2018, doi: 10.1038/s41586-018-0551-y.

[10] M. Xu, Y. Zhu, F. Pittalà, J. Tang, M. He, W. C. Ng, J. Wang, Z. Ruan, X. Tang, M. Kuschnerov, L. Liu, S. Yu, B. Zheng, and X. Cai, ‘Dual-polarization thin-film lithium niobate in-phase quadrature modulators for terabit-per-second transmission’, *Optica*, vol. 9, no. 1, pp. 61–62, 2022, doi: 10.1364/OPTICA.449691.

[11] S. Abel, F. Eltes, J. E. Ortmann, A. Messner, P. Castera, T. Wagner, D. Urbonas, A. Rosa, A. M. Gutierrez, D. Tulli, P. Ma, B. Baeuerle, A. Josten, W. Heni, D. Caimi, L. Czornomaz, A. A. Demkov, J. Leuthold, P. Sanchis, and J. Fompeyrine, ‘Large Pockels effect in micro- and nanostructured barium titanate integrated on silicon’, *Nature Materials*, vol. 18, no. 1, Art. no. 1, 2019, doi: 10.1038/s41563-018-0208-0.

[12] A. Messner, F. Eltes, P. Ma, S. Abel, B. Baeuerle, A. Josten, W. Heni, D. Caimi, J. Fompeyrine, and J. Leuthold, ‘Plasmonic Ferroelectric Modulators’, *Journal of Lightwave Technology*, vol. 37, no. 2, pp. 281–290, 2019, doi: 10.1109/JLT.2018.2881332.

[13] F. Eltes, C. Mai, D. Caimi, M. Kroh, Y. Popoff, G. Winzer, D. Petousi, S. Lischke, J. E. Ortmann, L. Czornomaz, L. Zimmermann, J. Fompeyrine, and S. Abel, ‘A BaTiO3-Based Electro-Optic Pockels Modulator Monolithically Integrated on an Advanced Silicon Photonics Platform’, *Journal of Lightwave Technology*, vol. 37, no. 5, pp. 1456–1462, 2019, doi: 10.1109/JLT.2019.2893500.

[14] D. Moor, J. Winiger, P. Ma, A. Messner, B. I. Bitachon, S. Abel, F. Eltes, J. Fompeyrine, and J. Leuthold, ‘>150 GHz Hybrid-Plasmonic $BaTiO_3$-On-SOI Modulator for CMOS Foundry Integration’, in *Frontiers in Optics + Laser Science 2021 (2021), paper FTh4D.2*, 2021, p. FTh4D.2. doi: 10.1364/FIO.2021.FTh4D.2.

[15] S. H. Wemple and M. DiDomenico, ‘Electrooptical and Nonlinear Optical Properties of Crystals’, in *Applied Solid State Science*, vol. 3, R. Wolfe, Ed. Elsevier, 1972, pp. 263–383. doi: 10.1016/B978-0-12-002903-7.50011-4.

[16] P. Girouard, P. Chen, Y. K. Jeong, Z. Liu, S. Ho, and B. W. Wessels, ‘Chi(2) Modulator With 40-GHz Modulation Utilizing $BaTiO_3$ Photonic Crystal Waveguides’, *IEEE Journal of Quantum Electronics*, vol. 53, no. 4, pp. 1–10, 2017, doi: 10.1109/JQE.2017.2718222.

[17] R. C. Miller, ‘Optical second harmonic generation in piezoelectric crystals’, *Applied Physics Letters*, vol. 5, no. 1, pp. 17–19, 1964, doi: 10.1063/1.1754022.

[18] S. Kazaoui, J. Ravez, C. Elissalde, and M. Maglione, ‘High frequency dielectric relaxation in $BaTiO_3$ derived materials’, *Ferroelectrics*, vol. 135, no. 1, pp. 85–99, 1992, doi: 10.1080/00150199208230015.

[19] K. Laabidi, M. D. Fontana, M. Maglione, B. Jannot, and K. A. Müller, ‘Indications of Two Separate Relaxators in the Subphonon Region of Tetragonal BaTiO 3’, *Europhysics Letters (EPL)*, vol. 26, no. 4, pp. 309–314, 1994, doi: 10.1209/0295-5075/26/4/012.

[20] M. P. McNeal, S.-J. Jang, and R. E. Newnham, ‘The effect of grain and particle size on the microwave properties of barium titanate ($BaTiO_3$)’, *Journal of Applied Physics*, vol. 83, no. 6, pp. 3288–3297, 1998, doi: 10.1063/1.367097.

[21] J. Hlinka, T. Ostapchuk, D. Nuzhnyy, J. Petzelt, P. Kuzel, C. Kadlec, P. Vanek, I. Ponomareva, and L. Bellaiche, ‘Coexistence of the Phonon and Relaxation Soft Modes in the Terahertz Dielectric Response of Tetragonal $BaTiO_3$, *Physical Review Letters*, vol. 101, no. 16, p. 167402, 2008, doi: 10.1103/PhysRevLett.101.167402.

[22] L. Lafone, T. P. H. Sidiropoulos, and R. F. Oulton, ‘Silicon-based metal-loaded plasmonic waveguides for low-loss nanofocusing’, *Optics Letters*, vol. 39, no. 15, pp. 4356–4359, 2014, doi: 10.1364/OL.39.004356.

[23] Yongqiang Shi, Lianshan Yan, and A. E. Willner, ‘High-speed electrooptic modulator characterization using optical spectrum analysis’, *Journal of Lightwave Technology*, vol. 21, no. 10, pp. 2358–2367, 2003, doi: 10.1109/JLT.2003.818162.

[24] J.-M. Brosi, C. Koos, L. C. Andreani, M. Waldow, J. Leuthold, and W. Freude, ‘High-speed low-voltage electro-optic modulator with a polymer-infiltrated silicon photonic crystal waveguide’, *Optics Express*, vol. 16, no. 6, pp. 4177–4191, 2008, doi: 10.1364/OE.16.004177.

[25] M. Burla, C. Hoessbacher, W. Heni, C. Haffner, Y. Fedoryshyn, D. Werner, T. Watanabe, H. Massler, D. L. Elder, L. R. Dalton, and J. Leuthold, ‘500 GHz plasmonic Mach-Zehnder modulator enabling sub-THz microwave photonics’, *APL Photonics*, vol. 4, no. 5, p. 056106, 2019, doi: 10.1063/1.5086868.